Electronic Supplementary Material (ESI) for Inorganic Chemistry Frontiers.

Supporting Information

Mixed lanthanide-organic frameworks with borono groups for colorimetric detection of excess fluoride levels in rivers

Hui Min,*[a] Zhuohang Zhu,[a] Meiyi Huang,[a] Junbao Zhou,[a] Nian Zhao,[a] and Peng Cheng*[b]

[a] Hubei Key Laboratory of Pollutant Analysis & Reuse Technology, College of Chemistry and Chemical Engineering, Hubei Normal University, Huangshi 435002, P. R. China.

[b] Department of Chemistry, Key Laboratory of Advanced Energy Material Chemistry, Frontiers Science Center for New Organic Matter, Haihe Laboratory of Sustainable Chemical Transformations (Tianjin), College of Chemistry, Nankai University, Tianjin 300071, P. R. China.

* Authors to whom correspondence should be addressed: minhui@hbnu.edu.cn and pcheng@nankai.edu.cn.

Table of content

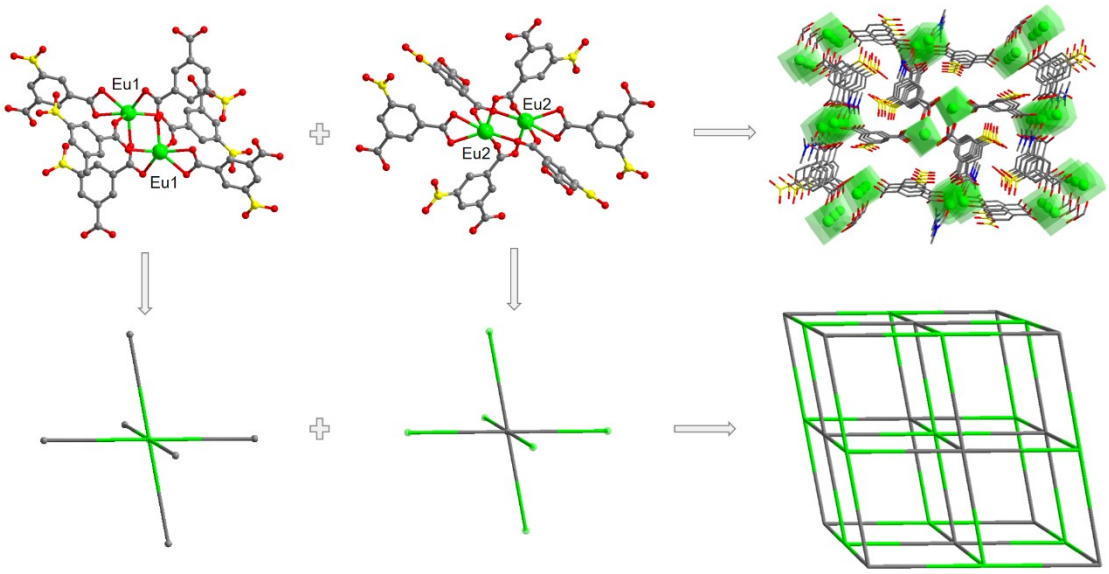

Fig. S1 The connected modes of binuclear {Eu_2} units and their simplified topological configuration.

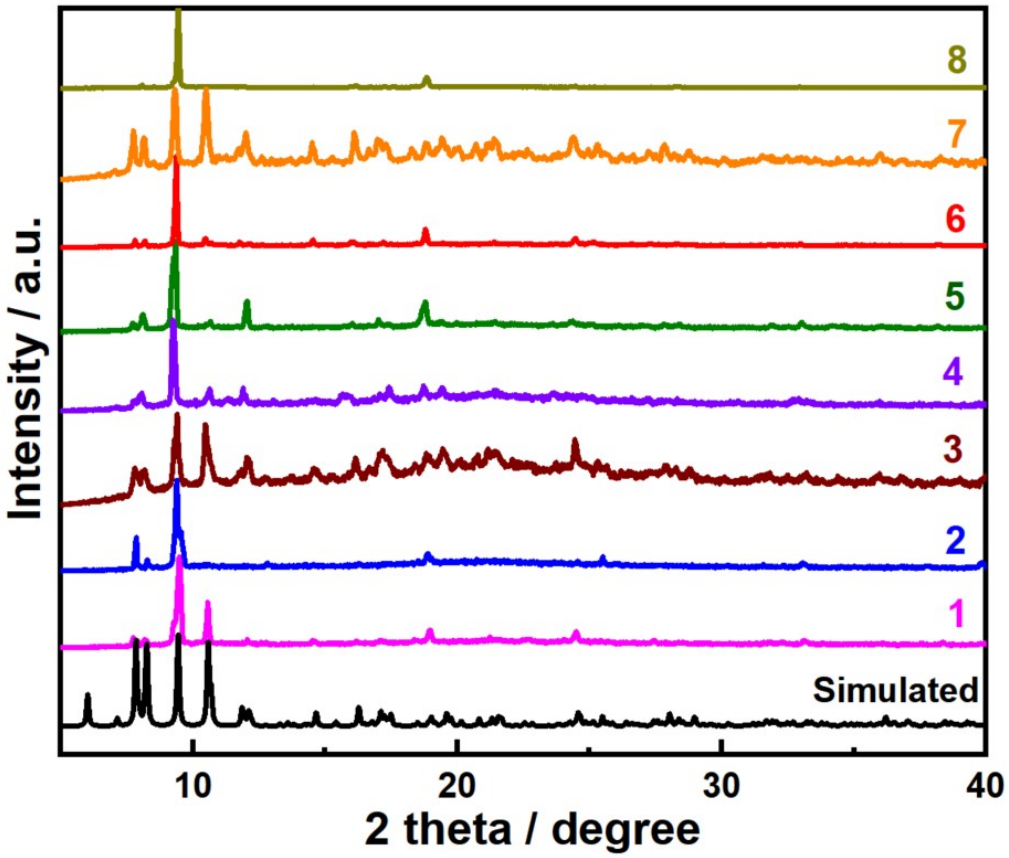

Fig. S2 PXRD patterns of as-synthesized **1** – **8** and the simulated one of **7**.

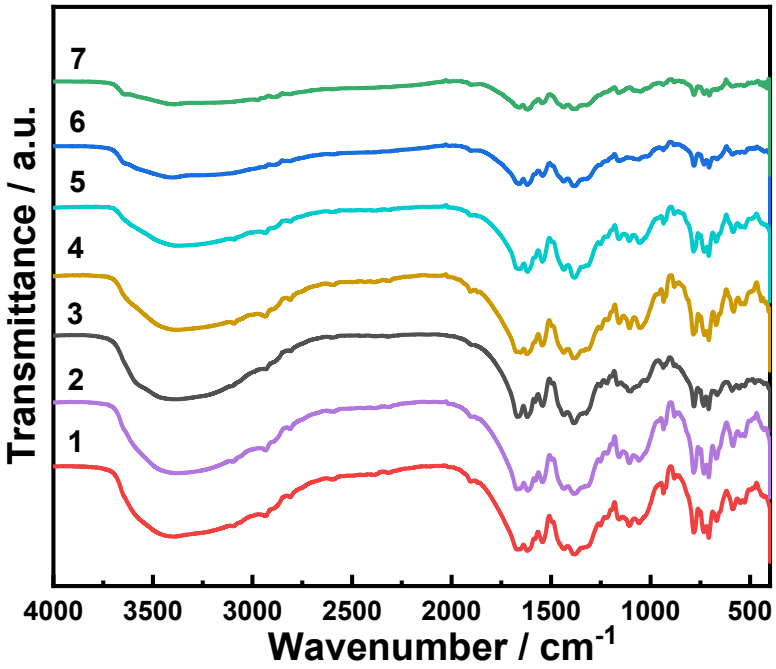

Fig. S3 IR curves of as-synthesized **1** – **7**.

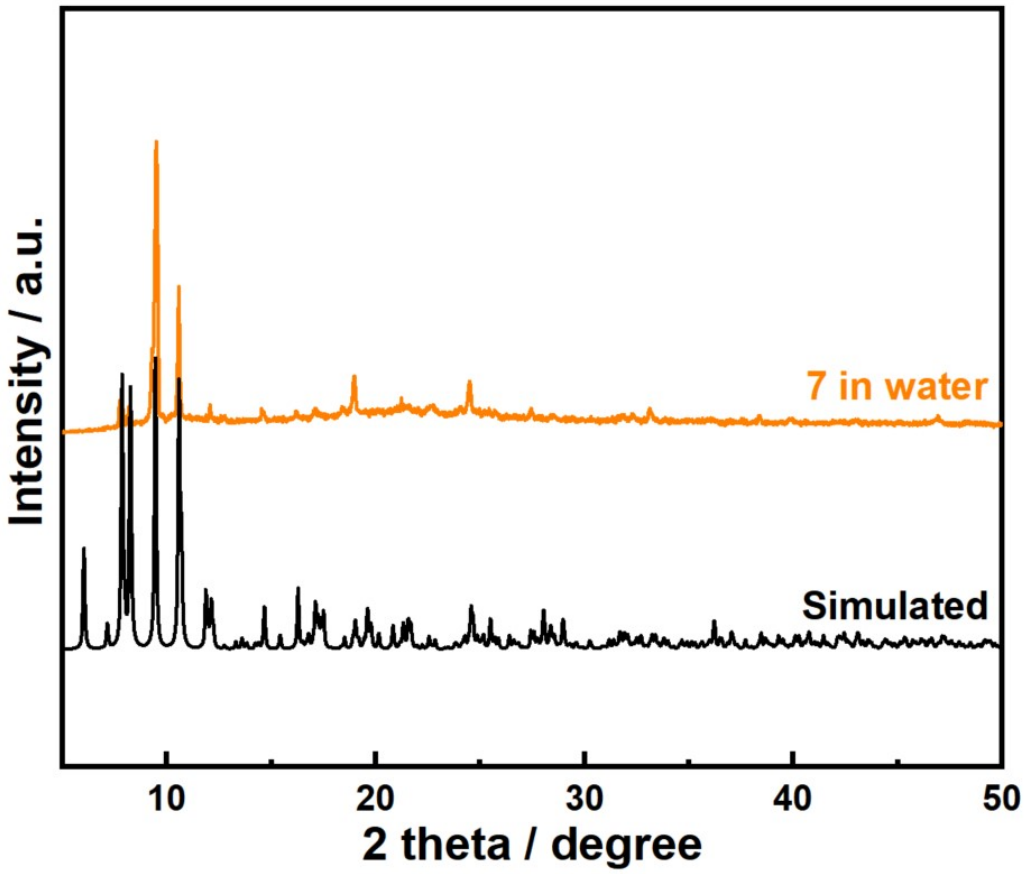

Fig. S4 PXRD patterns of **7** after immersing in water for 48 h and the simulated one of **7**.

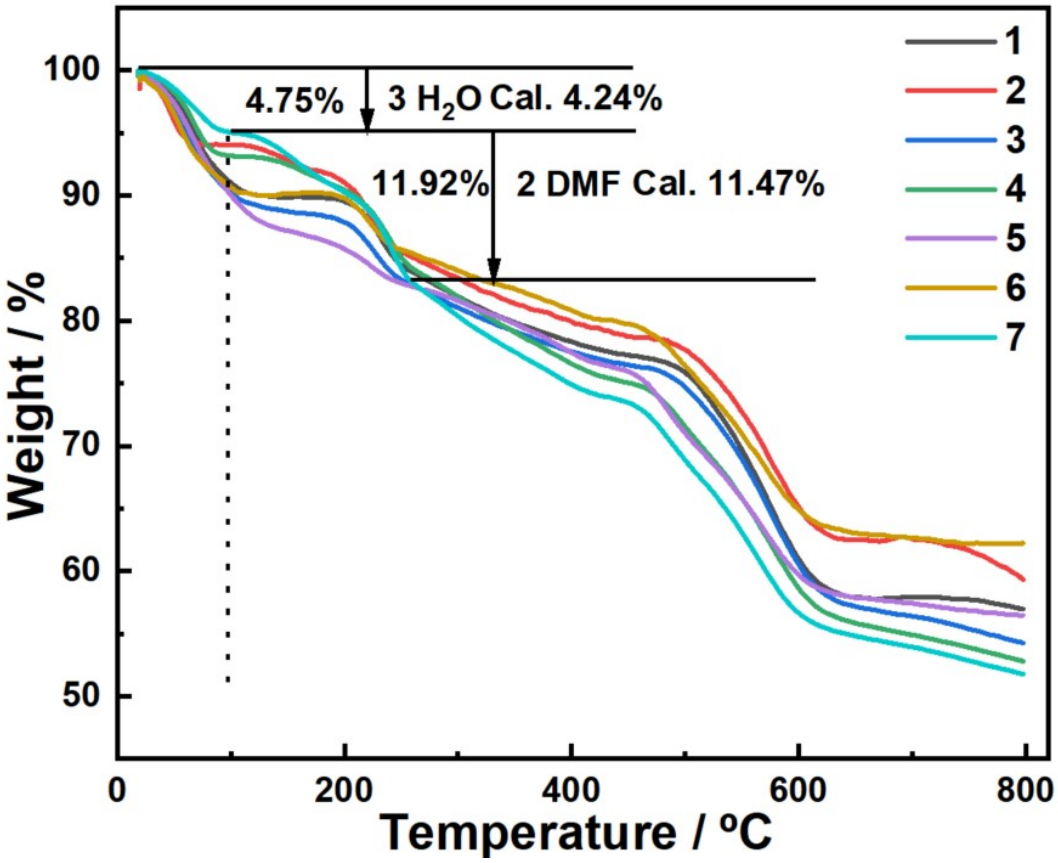

Fig. S5 TGA curves of as-synthesized **1** – **7**.

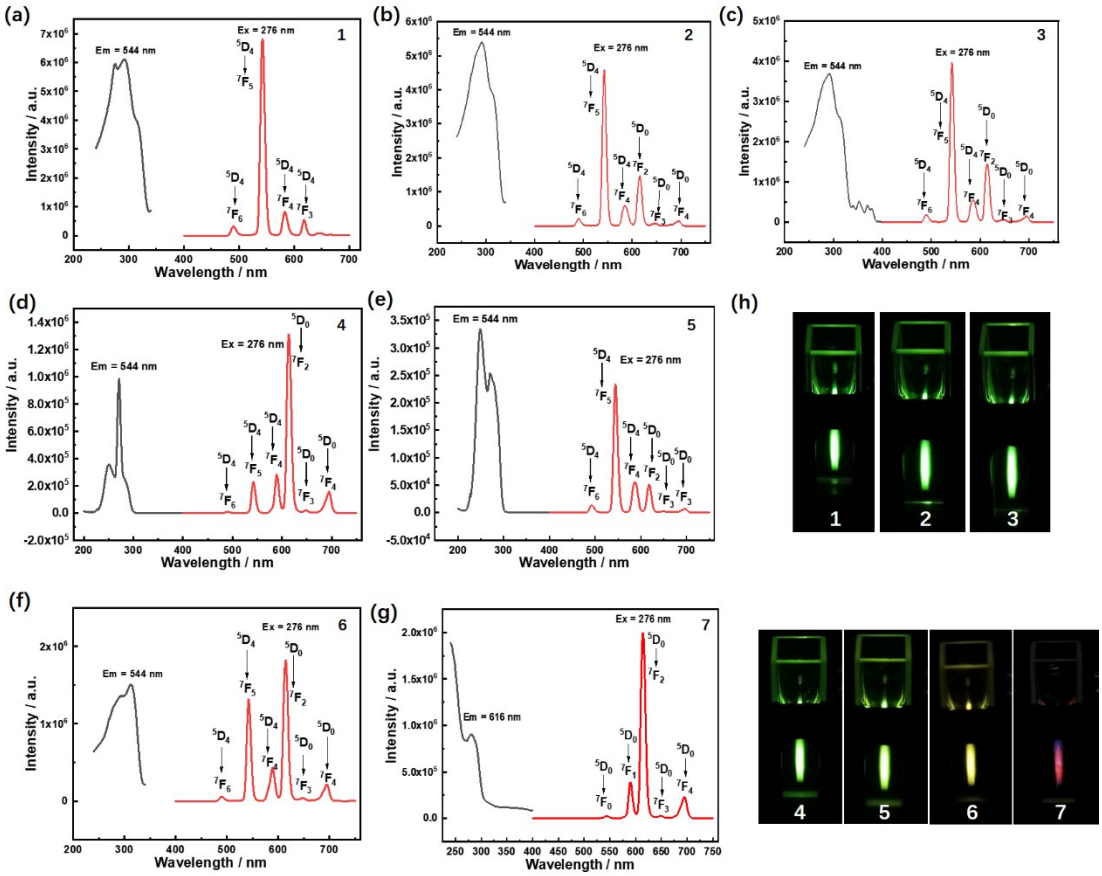

Fig. S6 Luminescence emission spectra (a – g) and luminescence pictures (h) of aqueous suspensions of **1** – **7**.

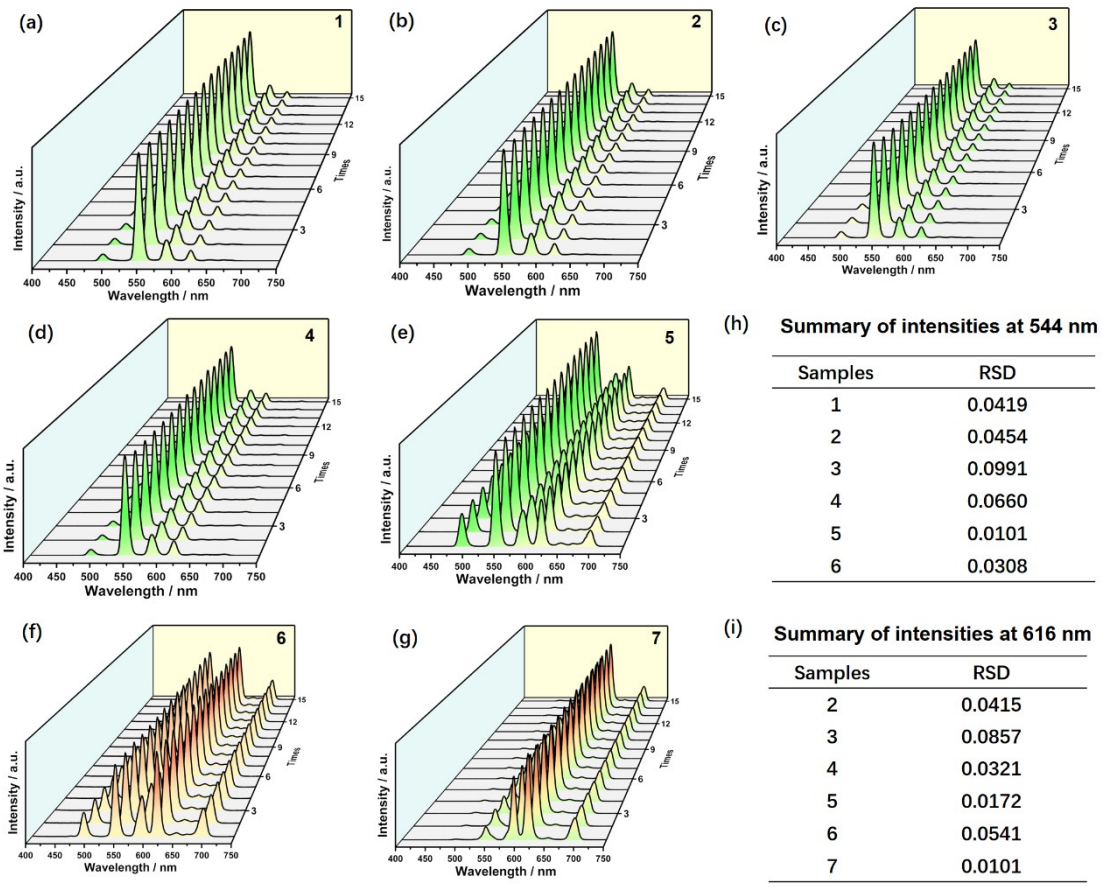

(h) **Summary of intensities at 544 nm**

Samples	RSD
1	0.0419
2	0.0454
3	0.0991
4	0.0660
5	0.0101
6	0.0308

(i) **Summary of intensities at 616 nm**

Samples	RSD
2	0.0415
3	0.0857
4	0.0321
5	0.0172
6	0.0541
7	0.0101

Fig. S7 Luminescent stability of aqueous suspensions of **1** – **7** for 15 min (a – g) and relative standard deviation (RSD) at 544 nm (h) or 616 nm (i).

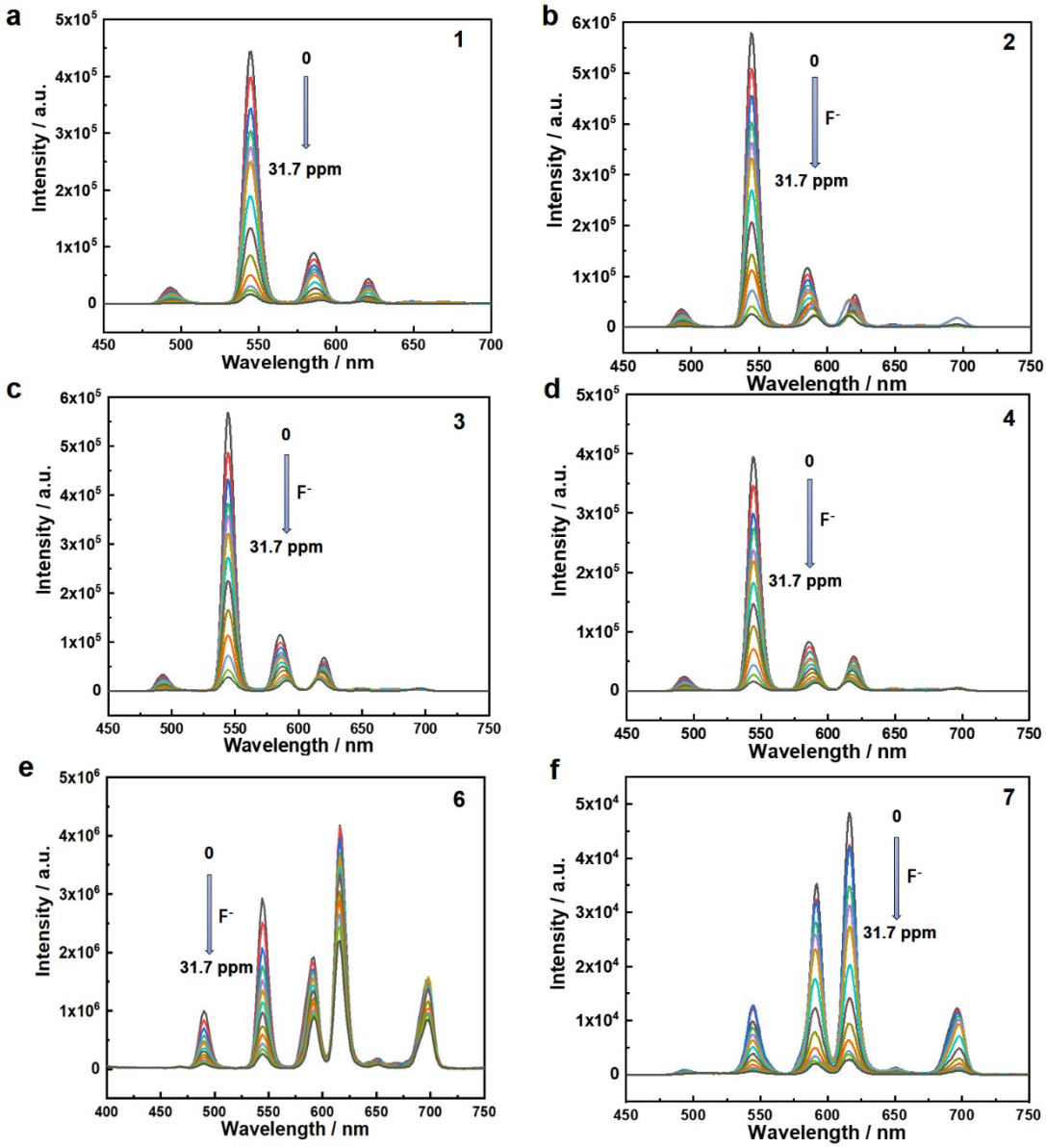

Fig. S8 Fluorescence spectra of **1** – **4** and **6** – **7** aqueous dispersions vary with F^- ion concentrations.

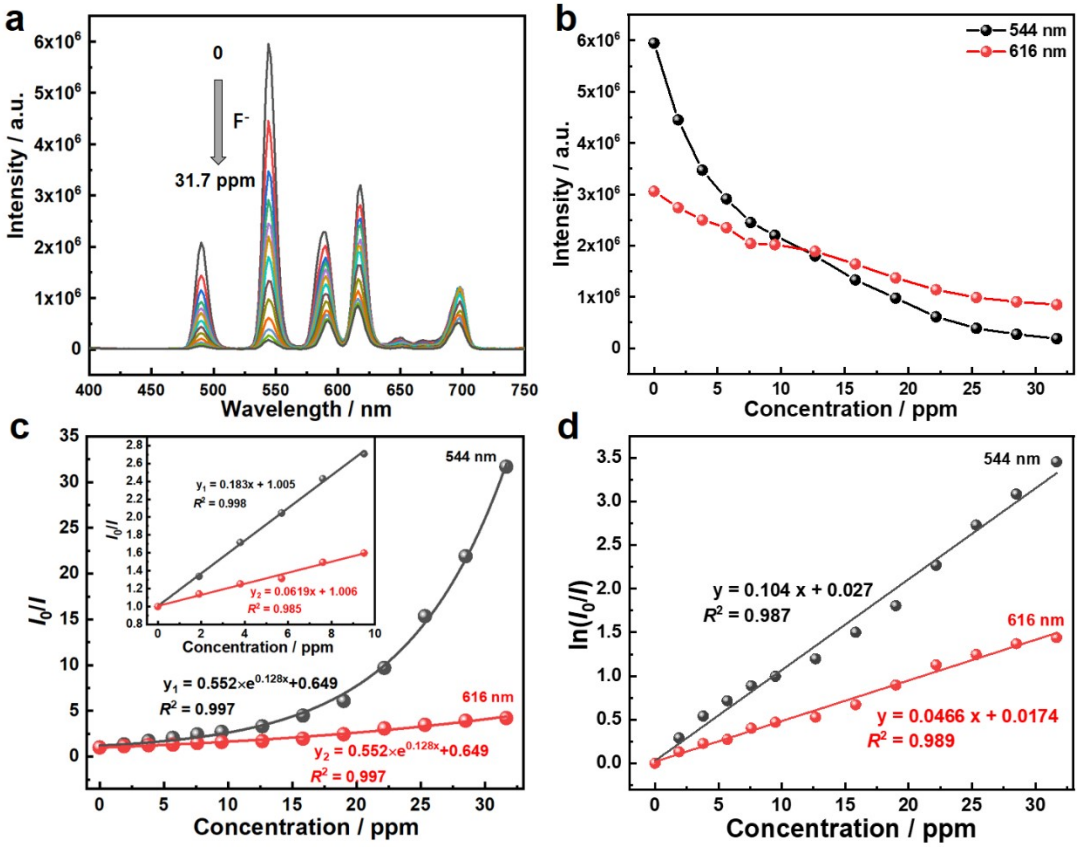

Fig. S9 Fluorescence response curves (a) and intensity (b) of **5** aqueous dispersions towards F^- with different concentrations. (c) Experimental S-V plots and the fitted result. Inset shows the linear fitting results at low concentration of F^- ions. (d) Linear fitting results of $\ln(I_0/I)$ and concentration.

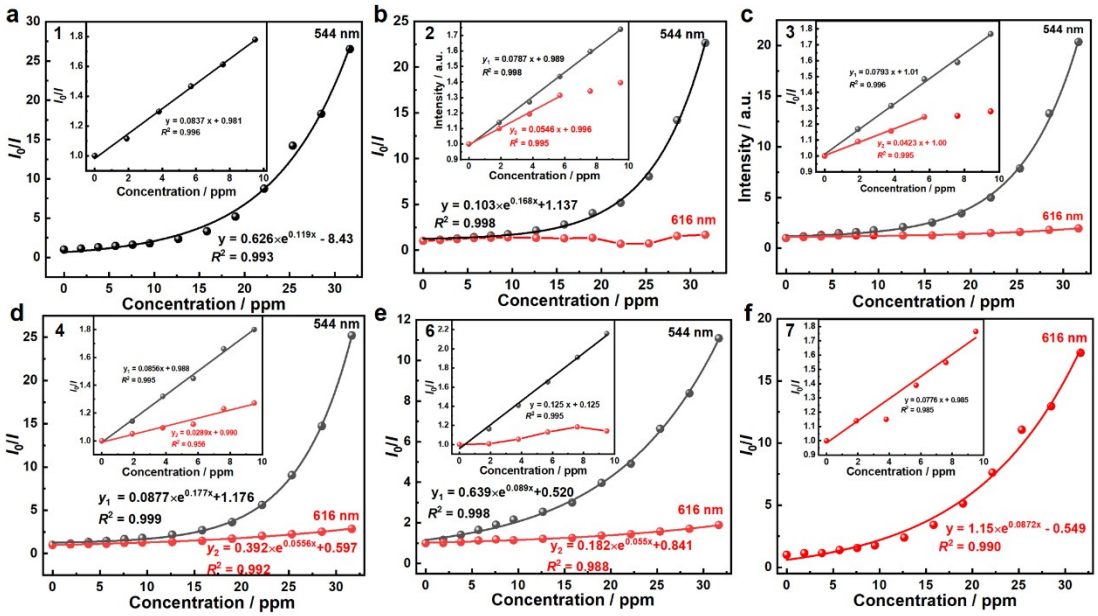

Fig. S10 S-V plots of **1** – **4** and **6** – **7** aqueous dispersions towards F^- ions with different concentrations, inset show the linear fit results at low concentration.

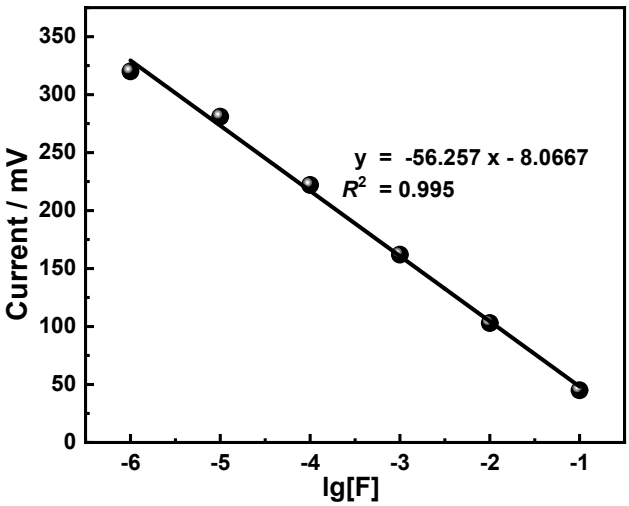

Fig. S11 Standard curve for F^- ion detection using F^- ion selective electrode.

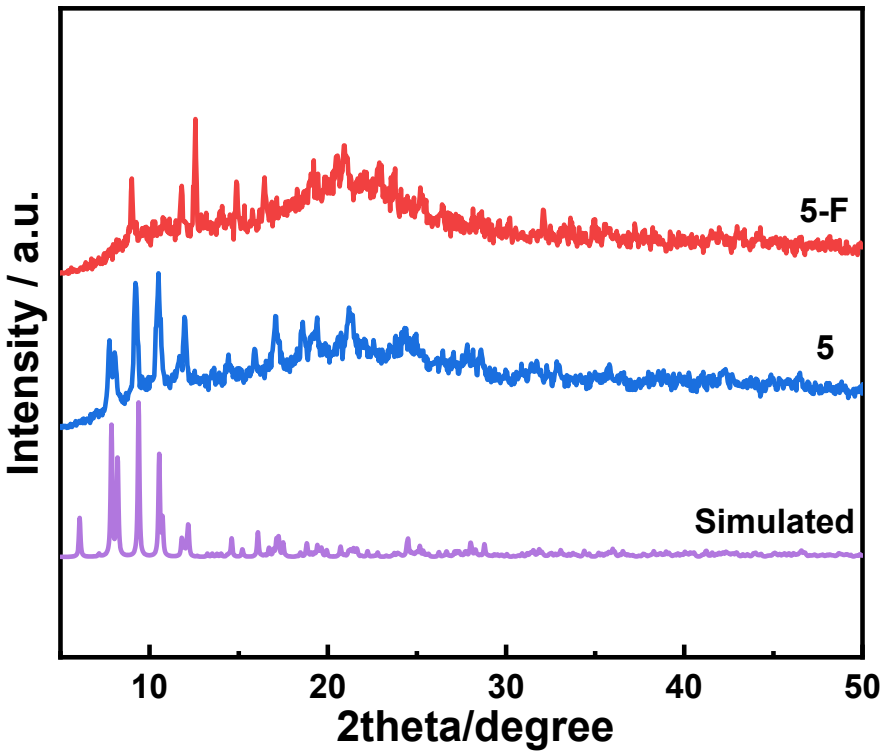

Fig. S12 PXRD patterns of **5** before and after treating with 30 ppm F^- ions.

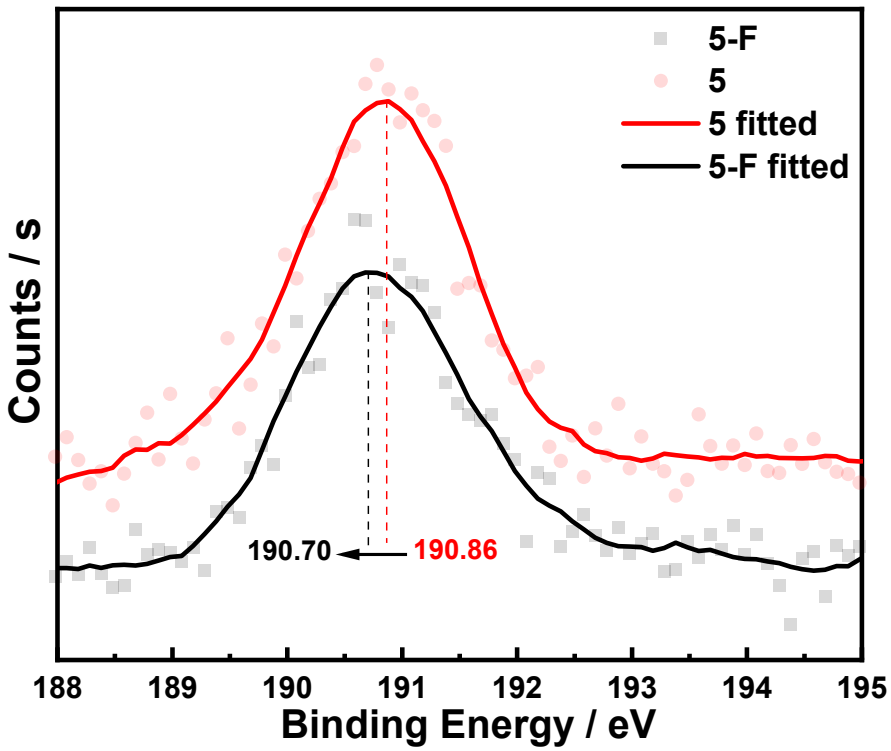

Fig. S13 XPS spectra of **5** before and after treating with F^- ions.

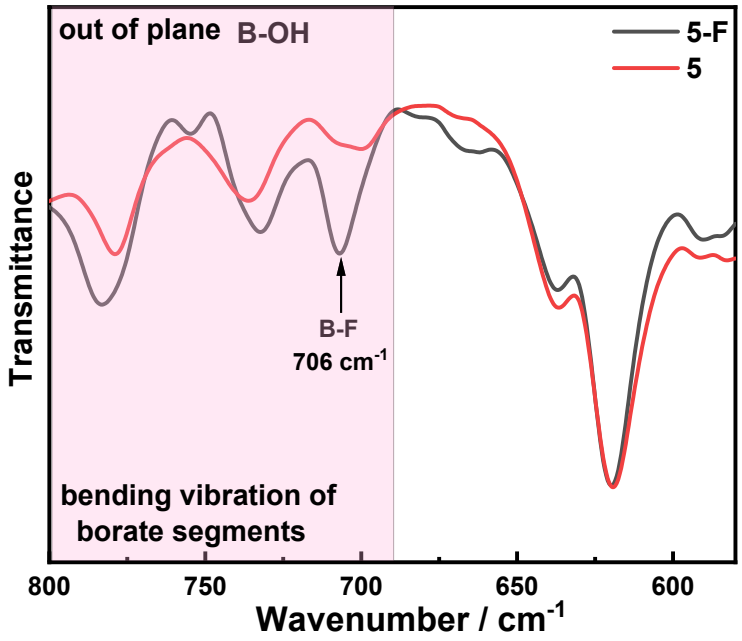

Fig. S14 IR curves of **5** before and after treating with F^- ions.

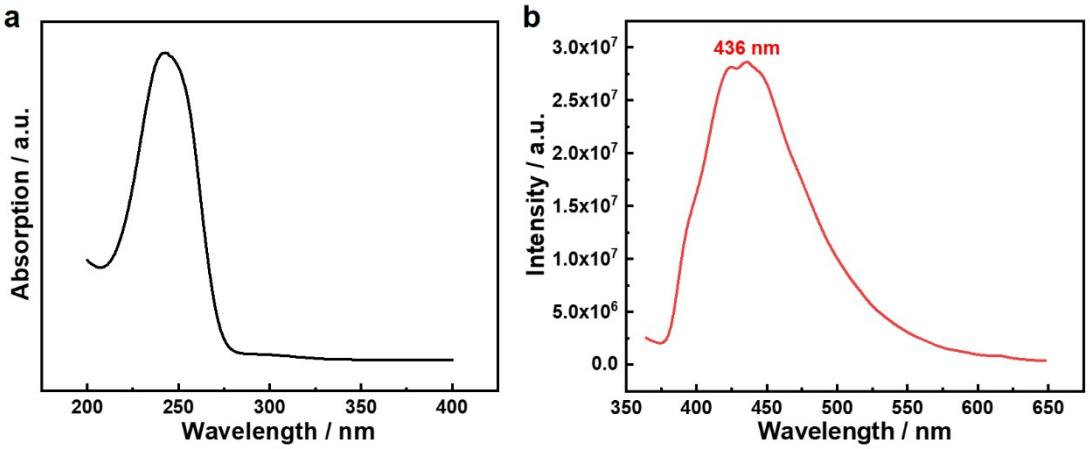

Fig. S15 (a) UV absorption spectrum of H_2BIPA and (b) 77 K phosphorescence spectrum of **8**.

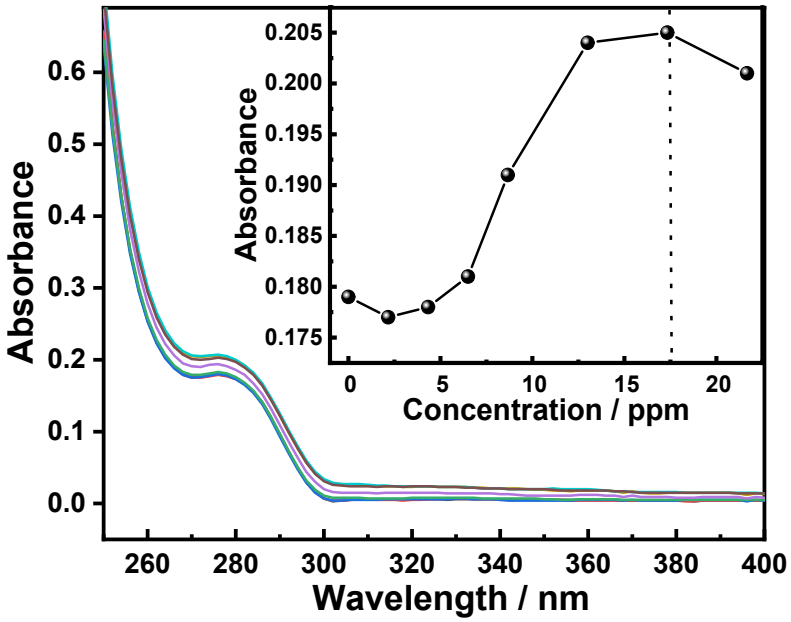

Fig. S16 Ultraviolet-visible absorption spectra of **5** aqueous dispersion vary with F^- ion concentrations, inset shows the absorbance at 278 nm at different concentration.

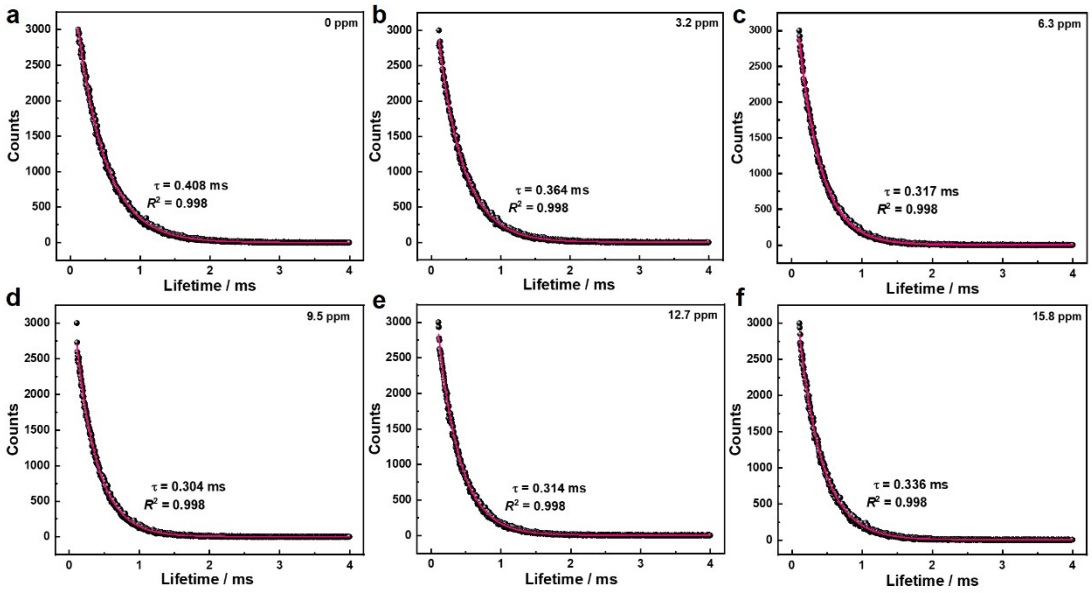

Fig. S17 Lifetimes at 544 nm of **5** aqueous dispersions towards F^- ions with different concentrations.

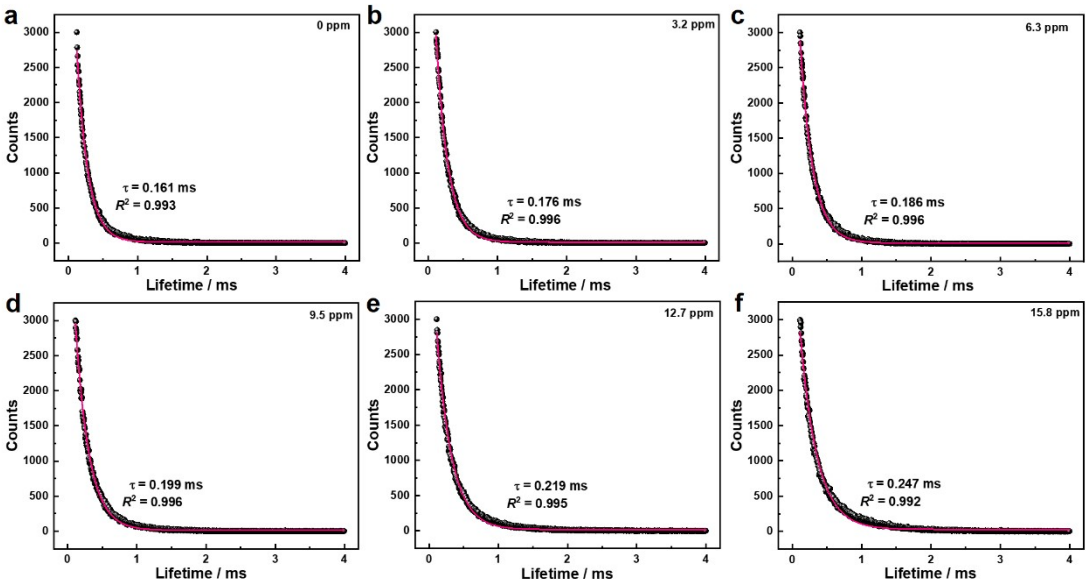

Fig. S18 Lifetimes at 616 nm of **5** aqueous dispersions towards F^- ions with different concentrations.

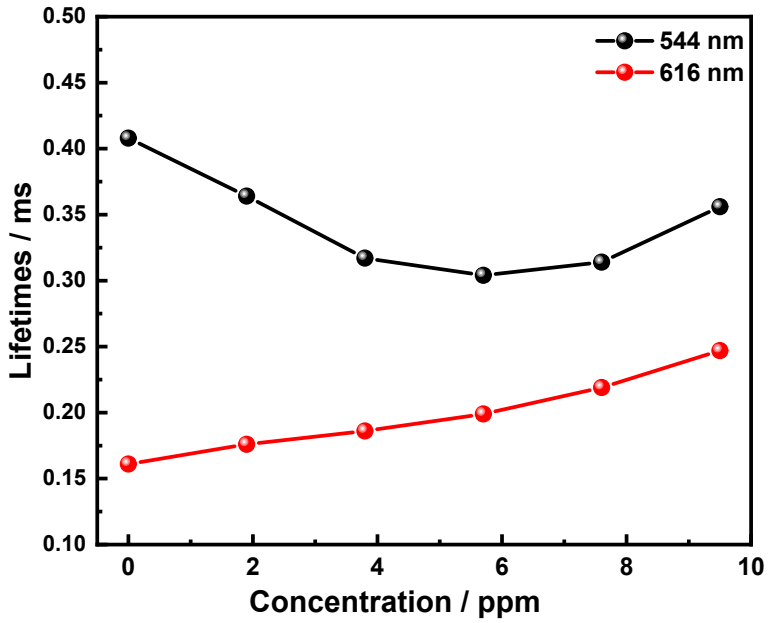

Fig. S19 Lifetimes at 544 nm and 616 nm of **5** aqueous dispersions towards F^- ions with different concentrations.

Table S1 EA and ICP-AES results for **1** – **7**.

Compounds	Addition/mL		EA results (%)			ICP-AES results	
	Tb^{3+}:Eu^{3+}	Elements	N	C	H	Tb	Eu
1	1.00:0.00	Calcd	3.26	30.77	3.89	1	-
		Found	2.93	30.93	4.34		
2	0.95:0.05	Calcd	3.27	30.79	3.89	0.94	0.06
		Found	3.09	30.65	4.04		
3	0.90:0.10	Calcd	3.27	30.82	3.89	0.86	0.14
		Found	3.43	30.40	4.10		
4	0.80:0.20	Calcd	3.27	30.82	3.89	0.85	0.15
		Found	2.74	30.48	4.35		
5	0.60:0.40	Calcd	3.28	30.89	3.90	0.66	0.34
		Found	2.99	30.62	4.01		
6	0.40:0.60	Calcd	3.28	30.95	3.91	0.48	0.52
		Found	3.12	30.97	4.20		
7	0.00:1.00	Calcd	3.30	31.11	3.93	-	1
		Found	3.23	31.30	4.04		

ICP-AES results show the normalized atomic ratio.

Table S2 Crystal data and structural refinement parameters for **7** and F@**7**.

Compounds	**7**	F@**7**
Formula	$C_{30}H_{40}B_3Eu_2N_2O_{25.5}$	$C_{30}H_{47}B_3Eu_2N_2O_{29}F_{0.25}$
Formula weight	1172.99	1256.79
Crystal system	triclinic	triclinic
Space group	*P-1*	*P-1*
a (Å)	12.771	12.670
b (Å)	14.199	14.235
c (Å)	15.899	16.014
α (°)	98.717	98.801
ß (°)	106.354	105.956
γ (°)	114.260	113.980
V (Å^3)	2401.4	2419.31
Z	2	2
D_x, g cm^{-3}	1.622	1.725
Mu, mm^{-1}	2.670	2.664
F(000)	1158.0	1248.0
GOF on F^2	1.052	1.014
R_{int}	0.0735	0.0473
$^aR_1$, $^bwR_2$ [$I \geq 2\ \sigma(I)$]	0.0685 / 0.1746	0.0410 / 0.1121
$^aR_1$, $^bwR_2$ [all data]	0.0981 / 0.1928	0.0549 / 0.1184
CCDC	2326600	2326601

$^aR_1 = \sum||F_o| - |F_c||/\sum|F_o|$; $^bwR_2 = [\sum w(F_o^2 - F_c^2)^2/\sum w(F_o^2)^2]^{1/2}$.

Table S3 Coordination configuration of the Eu1 and Eu2 calculated by *Shape 2.0*.

Ions	Abbreviation	Point group	Configuration	Deviation
Eu1	OP-8	D_{8h}	Octagon	30.131
	HPY-8	C_{7v}	Heptagonal pyramid	22.911
	HBPY-8	D_{6h}	Hexagonal bipyramid	15.803
	CU-8	O_h	Cube	11.456
	SAPR-8	D_{4d}	Square antiprism	1.728
	TDD-8	D_{2d}	Triangular dodecahedron	2.628
	JGBF-8	D_{2d}	Johnson gyrobifastigium J26	13.989
	JETBPY-8	D_{3h}	Johnson elongated triangular bipyramid J14	26.602
	JBTPR-8	C_{2v}	Biaugmented trigonal prism J50	1.882
	BTPR-8	C_{2v}	Biaugmented trigonal prism	0.993
	JSD-8	D_{2d}	Snub diphenoid J84	4.572
	TT-8	T_d	Triakis tetrahedron	11.859
	ETBPY-8	D_{3h}	Elongated trigonal bipyramid	22.823
Eu2	EP-9	D_{9h}	Enneagon	33.471
	OPY-9	C_{8v}	Octagonal pyramid	22.842
	HBPY-9	D_{7h}	Heptagonal bipyramid	16.220
	JTC-9	C_{3v}	Johnson triangular cupola J3	15.915
	JCCU-9	C_{4v}	JCCU-9	10.048
	CCU-9	C_{4v}	Spherical-relaxed capped cube	8.777
	JCSAPR-9	C_{4v}	Capped square antiprism J10	2.374
	CSAPR-9	C_{4v}	Spherical capped square antiprism	1.994
	JTCTPR-9	D_{3h}	Tricapped trigonal prism J51	3.286
	TCTPR-9	D_{3h}	Spherical tricapped trigonal prism	2.841
	JTDIC-9	C_{3v}	Tridiminished icosahedron J63	13.649
	HH-9	C_{2v}	Hula-hoop	8.064
	MFF-9	C_s	Muffin	0.981

Table S4 Performance summary of **1** – **7** toward F^- ions.

Sample	Sensitivity (ppm^{-1})		Limit of detection (ppm)	
	I_{544}	I_{616}	I_{544}	I_{616}
1	0.0837	-	1.50	-
2	0.0787	0.0546	1.73	2.28
3	0.0793	0.0423	3.74	7.03
4	0.0856	0.0289	2.31	3.33
5	0.183	0.0619	0.166	0.83
6	0.125	0.0190	0.739	8.54
7	-	0.0776		9.15

Table S5 Spike-and-recovery experiments of **5** towards F^- ions in water samples from the Yangtze River.

Methods	Samples	Found (ppm) [a]	Added (ppm)	Found (ppm) [b]	Recovery	RSD
This work	1	0.52	12.7	12.9	97.4%	2.3%
	2	0.75	12.7	13.2	98.0%	
	3	0.28	12.7	12.6	97.0%	
F- ion selective electrode	1	0.79	12.7	11.0	82.2%	8.5%
	2	0.82	12.7	13.0	96.0%	
	3	0.72	12.7	12.5	93.1%	

[a] direct measurement of F^- ion content in samples; [b] F^- ion content in samples after adding standard solution.

Table S6 Lifetime at 544 nm and 616 nm of **5** aqueous dispersions towards F^- ions with different concentrations.

Concentration (ppm)	Lifetime / ms	
	544 nm	616 nm
0	0.408	0.161
1.9	0.364	0.176
3.8	0.317	0.183
9	0.304	0.199
12	0.314	0.219
15	0.356	0.247